

The intertropical convergence zone modulates intense hurricane strikes on the western North Atlantic margin

Peter J. van Hengstum^{1,2,*}, Jeffrey P. Donnelly², Patricia L. Fall³, Michael R. Toomey⁴, Nancy A. Albury⁵, Brian Kakuk⁶

1. Texas A&M University at Galveston, Department of Marine Sciences, Galveston, Texas, 77554

2. Texas A&M University, Department of Oceanography, College Station, Texas, 77843

3. Woods Hole Oceanographic Institution, Department of Geology and Geophysics, Woods Hole, Massachusetts, 02543, USA

4. University of North Carolina Charlotte, Department of Geography and Earth Sciences, Charlotte, North Carolina, 28223, USA

5. U.S. Geological Survey, Eastern Geology and Paleoclimate Science Center, Reston, VA, 20192.

6. Antiquities, Monuments, and Museums Corporation/National Museum of The Bahamas, PO Box EE-15082, Nassau, The Bahamas

7. Bahamas Underground, Marsh Harbour, Abaco Island, The Bahamas.

*Corresponding author: vanhenp@tamug.edu

ABSTRACT

Most Atlantic hurricanes form in the Main Development Region between 9°N to 20°N along the northern edge of the Intertropical Convergence Zone (ITCZ). Previous research has suggested that meridional shifts in the ITCZ position on geologic timescales can modulate hurricane activity, but continuous and long-term storm records are needed from multiple sites to assess this hypothesis. Here we present a 3000 year record of intense hurricane strikes in the northern Bahamas (Abaco Island) based on overwash deposits in a coastal sinkhole, which indicates that the ITCZ has likely helped modulate intense hurricane strikes on the western North Atlantic margin on millennial to centennial-scales. The new reconstruction closely matches a previous reconstruction from Puerto Rico, and documents a period of elevated intense hurricane activity on the western North Atlantic margin from 2500 to 1000 years ago when paleo precipitation proxies suggest that the ITCZ occupied a more northern position. Considering that anthropogenic warming is predicted to be focused in the northern hemisphere in the coming century, these results provide a prehistoric analog that an attendant northern ITCZ shift in the future may again return the western North Atlantic margin to an active hurricane interval.

Introduction

Most intense North Atlantic hurricanes form just poleward of the Intertropical Convergence Zone (ITCZ) in the Main Development Region (MDR, 9°N and 20°N)¹, where the dominant local environmental factor influencing hurricane activity is wind shear between the upper and lower troposphere². The ITCZ is a zone of deep convection and heavy precipitation that is generated by convergence of the trade winds, and it migrates between 9°N and 2°N in response to seasonal sea surface temperature (SST) warming³. In the tropical Atlantic, the Atlantic Meridional Mode (AMM) is the dominant mode of ocean-atmospheric interaction between SSTs and low-level winds⁴. The AMM is associated with an anomalous meridional sea surface temperature gradient across the mean ITCZ latitude and a cross-gradient atmospheric boundary layer flow, which shifts the ITCZ towards the warmer hemisphere⁴⁻⁶. A positive phase of the AMM is associated with a strong meridional SST gradient, a northward shift in the ITCZ, and decreased vertical wind shear in the tropical Atlantic⁷. As such, meridional ITCZ displacements and intense hurricane landfalls on the western North Atlantic margin over millennial timescales could potentially co-vary during more positive AMM-like states of the tropical Atlantic. The Little Bahama Bank is an important geographic location for testing this hypothesis because it is located between sites on the western Atlantic margin in the Caribbean region⁸ and the US Eastern Seaboard⁹ where continuous hurricane reconstructions have been previously generated.

Blackwood Sinkhole is located 220 m inland from the shoreline on the eastern shore of Great Abaco in the northern Bahamas (Fig. 1; 26.79°N, 77.42°W). Sinkholes and blueholes are ubiquitous on the Bahamian landscape, which develop from the subsurface dissolution and subsequent collapse of limestone bedrock¹⁰. The sediments within these karst basins are well-known archives of Holocene paleo climate records on carbonate landscapes¹¹⁻¹⁷. Great Abaco is a low-lying carbonate island on the Little Bahama Bank, which has a typical tidal range of ~1 m. A wetland is currently adjacent to the sinkhole, and no streams discharge into the site (Figs. 1,2). This groundwater-fed coastal basin is stratified, with anoxic saline groundwater located from 15 m below sea level to its maximum at 40 m below sea level (Fig. 2, S1). Since 1851 Common Era (CE), 42 hurricanes have passed within 65 nm of Blackwood Sinkhole. Sixteen of these storms were major hurricanes (Category 3, 4, or 5 on the Saffir-Simpson Scale), and the majority of these (88%) formed in the central and eastern MDR¹⁸.

The Sediment Record

Two sediment push cores were collected from Blackwood Sinkhole using advanced technical scuba diving procedures. The sediment cores terminated on carbonate gravel, above which was laminated gyttja (~1 mm to 1 cm laminae) with discrete coarse-grained sedimentary layers (Fig. 3). Both laminations and coarse layers could be visually correlated between cores (e.g., BLWD-C1: 40 to 44 cm, BLWD-C2: 11 to 16 cm; Fig. 3), except for two non-laminated units of coarse terrestrial organic matter in BLWD-C1 (20 to 35 cm, and 84 to 93 cm, Fig. 3). Since these chaotic units likely represent slump events along the sinkhole periphery, the periodicity of coarse-grained sedimentation was examined further by developing a detailed age model from BLWD-C2 (See Online Supplementary Material). Episodic sedimentation occurred in BLWD-C2 from 7622 to 7494 Cal yrs BP₁₉₅₀ (2σ , 0.989 probability, 122 cm core depth) until 2960 to 2838 Cal yrs BP (2σ , 0.9089 probability, 109 cm core depth, Fig. S2). However, the sedimentation rate was nearly constant through the late Holocene (3000 years to present) from 109 to 0 cm (least squares regression: $r^2 = 0.991$, $n = 11$ dates, 0.3 to 0.6 mm yr⁻¹). Coarse-grained sedimentation was examined in contiguous 5 mm sediment samples downcore, which provides a record where each 5 mm sample represents 16 to 32 years over the late Holocene. Pollen was also analyzed in BLWD-C2 in 1 cm intervals downcore to further examine any relationship between coarse sedimentation into the sinkhole and vegetation changes on the adjacent terrestrial landscape.

The most obvious stratigraphic features are sand layers concentrated during discrete time intervals (Figs. 2, 3A): (a) 178 to 19 Cal yrs BP, (b) 438 to 387 Cal yrs BP, (c) 2486 to 1125 Cal yrs BP, and one event occurs at 2883 Cal yrs BP. Only mangrove invertebrates (e.g., gastropods, bivalves) and angular carbonate particles compose the sand layers. In contrast, rounded marine bioclasts and reef-dwelling foraminifera are abundant in the adjacent modern beach sediment ($n = 5$: mean 83% *Archaias*, Fig. S3). As such, the coarse sediment particles deposited at BLWD-C2 are most likely derived from the adjacent terrestrial and mangrove environments.

Local flooding combined with overwash from intense hurricane surge (\geq category 3) most likely caused deposition of the coarse-grained horizons in Blackwood Sinkhole. Both numerical models^{19,20} and field observations^{21,22} indicate that since groundwater levels in low-lying unconfined aquifers are intimately linked to sea-level change and precipitation, landscape flooding often occurs during intense hurricane events. Indeed, the uppermost sand layer from 0.5 to 1.0 cm

depth was deposited between 1981.7 and 2008.8 CE (2σ) when six hurricanes struck eastern Abaco, but only two generated local surge and flooding. Hurricane Floyd originated as an African easterly wave²³ that made landfall on 14 September 1999 as a weakening category 4 event, with sustained 225 km/hr winds, +2 m storm surge and widespread flooding and destruction²⁴. Hurricane Jeanne also originated as an African wave²⁵, striking eastern Abaco Island on 25 September 2004 as a category 3 event with sustained winds up to 185 km hr⁻¹. Considering the uncertainty of our age model it is difficult to precisely attribute the event bed from 0.5 to 1.0 cm to a particular event, but the age of the deposit is consistent with deposition either from Floyd or Jeanne. Older coarse-grained layers deposited in the last 150 years may relate to other Bahamian hurricane disasters (e.g., 1932 CE hurricane, category 5), but uncertainty in the age model prevents confident association of other coarse-grained peaks to specific storm events. Based on the uppermost event, however, it appears that intense hurricane strikes with surge and flooding exceeding 2 m above sea level are responsible for event bed deposition ($>20 \text{ mg cm}^{-3}$) at this core locale.

The record does contain limitations. Multiple intense surge events occurring on sub-decadal timescales cannot be differentiated because of the sampling strategy (analytical time averaging) and sedimentation rate, and multiple types of storms can likely generate +2 m surges (e.g.,²⁶). Also, the magnitude of coarse fraction sedimentation from one core alone cannot be used to infer hurricane intensity as multiple parameters (e.g., radius of maximum winds, storm translational velocity, local sediment budget and coastal geometry) can influence the lateral variability of a tempestite in the subsurface²⁷. At the core site of BLWD-C2, however, varying coarse-grained sedimentation into Blackwood Sinkhole can be used to indicate active versus quiescent intervals of hurricane activity through time. Furthermore, the current geometry of the site was likely similar over the time that this sediment archive was accumulating, given the modest rates of regional sea-level rise during the late Holocene²⁸ and the sinkhole's structural geology.

Discussion

Climate forcing

The most significant result of the Blackwood reconstruction is the contrast between pronounced active versus quiescent intervals of intense hurricane landfalls based on event bed deposition, which closely matches previous evidence for intense hurricane strikes at Laguna Playa

Grande in Puerto Rico (LPG, 18.09°N, 65.49°W, compare Figs. 4A and 4B)⁸. Relying on historical intense hurricane climatology for the last 164 years¹⁸, both LPG and Blackwood are predominantly vulnerable to storms forming in the central MDR. The concordance between the signal at LPG and Blackwood suggests that we sampled a similar population of intense hurricanes striking the western North Atlantic margin over the last 3000 years, which most likely originated in the central MDR.

Woodruff et al.²⁹ demonstrated that the active interval from 2500 to 1000 Cal yrs BP was at least partially driven by changes in regional hurricane climatology, despite lower sedimentation rates in the older part of the LPG reconstruction. Furthermore, quiescent intervals observed at LPG were statistically unlikely under current climatological conditions, and could not be replicated even when climate conditions for a hurricane downscaling model were forced into a constant El Niño state²⁹, which is thought to limit Atlantic hurricane activity³⁰. Given the constant sedimentation rate in the record from Blackwood Sinkhole, and its replication of the LPG reconstruction, the pronounced oscillation between active versus quiescent periods of intense hurricane activity is most likely driven by broadscale climate features operating on multi-decadal or greater timescales, not interannual forcing like El Niño/Southern Oscillation.

In the modern climate, positive (negative) Atlantic Meridional Mode (AMM) phases are associated with a northward (southward) shift of the ITCZ, which reduces (increases) vertical shear in the MDR by moving the ascending branch of the Hadley circulation slightly northwards (southwards)^{6,7,31}. In turn, a more northerly (southerly) position of the ITCZ enhances (diminishes) cyclogenesis in the eastern tropical North Atlantic (northeastern seaboard)⁷. Given that the AMM is excited on multi-decadal timescales by the Atlantic Multidecadal Oscillation³², a multi-decadal hurricane reconstruction may provide insight into likely instances of more common positive AMM-like states of the tropical Atlantic, and an attendant northern ITCZ displacement. During the Holocene, the temperature contrast between the Northern and Southern Hemisphere extratropics correlates well to Holocene-scale records of global hydroclimate and meridional ITCZ displacements^{3,33}, which can be used to probe the long-term correlation between ITCZ migrations and western North Atlantic margin hurricane landfalls.

No intense hurricane is recorded at Blackwood from 2900 to 2500 Cal yrs BP, which is likely the tail-end of the quiescent period previously observed at LPG from 3800 to 2500 Cal yrs BP. This quiescent period is coeval with proxy-based evidence for a more southerly position of the

ITCZ. For example, the temperature contrast between the extratropics in the Northern and Southern hemispheres suggests a more southern ITCZ position (Fig. 4D), which correlates well with terrestrial proxies of discharge into the Cariaco Basin³⁴ and the Indian Monsoon³. Elsewhere, the stable carbon isotopic values preserved in a speleothem from Cold Air Cave in Northeastern South Africa are thought to represent the regional proportion of C₃ vegetation (woodland savannas) versus C₄ vegetation (grasses, aridity-adapted) on the landscape related to regional aridity³⁵. The negative carbon isotopic excursion from 2900 to 2500 Cal yrs BP in Cold Air Cave indicates C₃ vegetation expansion, which suggests increased regional moisture delivery from a more southerly ITCZ in Africa (Fig. 4E). Similarly, Laguna Pallcacocha in Ecuador documents a decrease in intense precipitation events at this time (Fig. 4F)³⁶. Previously, the Laguna Pallcacocha record was interpreted as a proxy for only El Niño-driven flooding events^{8,36}, but here we suggest that increases in magnitude and frequency of red-hued beds deposited in Laguna Pallcacocha are also significantly impacted by southern ITCZ displacements.

From 2500 to 1000 Cal yrs BP, the North Atlantic experienced an interval of intense hurricane activity. This interval is coeval with paleoclimate evidence for a more northern ITCZ position relative to present, but not as far north as during the middle Holocene (Fig. 4D). Both Blackwood and LPG document this active interval, and hurricane-mediated export of coarse-grained sediment off the Grand Bahama Bank also increased³⁷. The tail-end of this active interval is observed at Salt Pond, Massachusetts (Fig. 4C), where increased intense hurricane landfalls occur between 1700 and 900 Cal yrs BP⁹. Concurrent with the onset of this active interval is a prominent increase in the temperature contrast between the Northern and Southern Hemisphere extratropics at 2500 Cal yrs BP, which suggests an abrupt northerly displacement of the ITCZ (Fig. 4D). This begins a period of Caribbean aridity relative to the middle Holocene as inferred from terrestrial vegetation in both Hispaniola³⁸⁻⁴⁰ and Andros¹⁵, C₄ plants expanded in South Africa³⁵, and decreased intense precipitation events at Laguna Pallcacocha (Fig. 4G). Given the rapid ~1.5°C warming observed in the eastern equatorial Atlantic during this interval⁴¹, oceanographic conditions would likely have been conducive for cyclogenesis. These records collectively suggest an abrupt shift to a more northerly ITCZ position from 2500 to 1000 Cal yrs BP, which would have favored cyclogenesis in the central MDR by reducing vertical wind shear, and increasing the likelihood of intense hurricane strikes in the western North Atlantic.

At 1000 Cal yrs BP, intense hurricane activity decreased in the western North Atlantic margin as evidenced at Blackwood, LPG, and Salt Pond. Previously completed statistical models based on ocean-atmospheric forcing of hurricane activity also projected a decrease in Atlantic hurricane activity after 1000 Cal yrs BP⁴². As discussed elsewhere⁴³, poor definition of the ITCZ position in the expansive Amazon basin partly explains observed differences between the Ti-runoff proxy into the Cariaco Basin and other records of South American precipitation anomalies during the last millennium. However, a southern ITCZ displacement at 1000 Cal yrs BP could have increased precipitation and resultant accumulation rates of the Quelccaya Ice Cap⁴³; allowed C₃ vegetation to expand in South Africa³⁵, and increased the likelihood of extreme precipitation events at Laguna Pallcacocha in Ecuador³⁶. Further north, a southern displacement of the ITCZ at 1000 Cal yrs BP likely increased aridity at multiple sites in the northern subtropics such as in the Yucatan⁴⁴, Dominican Republic⁴⁵, and Cuba⁴⁶, which could have decreased cyclogenesis in the MDR.

Late Holocene terrestrial vegetation changes in Abaco, reconstructed from pollen that was also preserved in BLWD-C2, provides further evidence for regional precipitation changes that are likely associated with meridional ITCZ displacements. Modern Bahamian precipitation is generally characterized by a latitudinal precipitation gradient⁴⁷, in which only the northern islands are sufficiently mesic to currently support *Pinus* forests (Abaco, Grand Bahamas, Andros, and New Providence). Bahamian islands further to the south are more arid, in part due to their close proximity to regional low-level atmospheric subsidence between the northeasterlies and anticyclonic flow⁴⁷. Furthermore, seasonal intensification of the subtropical ridge during boreal summer decreases Bahamian rainfall⁴⁸ by increasing subsidence and intensifying the easterlies, creating the mid-summer drought. These atmospheric processes are necessarily linked to displacements of the ITCZ given their spatial relationship with the Hadley Cell⁴⁹.

A wholesale change in regional moisture balance must have occurred at ~1000 Cal yrs BP when Abaconian forests transitioned from arid-adapted palms (Arecaeae) and tropical hardwoods (primarily *Bursera*, *Metopium*, Myrtaceae), to centennial-scale oscillations between the more mesic *Pinus caribaea* and *Conocarpus erectus* (buttonwood) in the last millennium. *Pinus* (pine) forests only became established on the northern Bahamian landscape ~700 years ago, based on pollen reconstructions from Abaco Island (Fig. 4H) and on nearby Andros Island¹⁵. The abrupt vegetation changes beginning at 1000 Cal yrs BP are also coincident with a loss of Abaco's

reptile-dominated terrestrial food webs⁵⁰, and perhaps other mammals⁵¹. The earliest human remains in the northern Bahamas date between 1050 and 920 Cal yrs BP⁵², but the concurrent expansion of *Pinus* in Andros¹⁵ and Abaco at ~700 Cal yrs BP suggests a synchronous regional response to hydroclimate change. Perhaps modest rates of late Holocene sea-level rise expanded suitable habitat for *C. erectus* in the wetlands adjacent to Blackwood sinkhole over the last 1500 years, but not the observed rapid centennial-scale oscillations in the dominance between coastal mangroves versus interior species (pines, hardwoods) that begins at 1000 Cal yrs BP. Prior to 1000 Cal yrs BP, a more northerly positioned ITCZ could have shifted the zone of regional subsidence between the easterlies and anticyclonic flow northwards, in turn promoting a more arid northern Bahamian region.

The southern displacement of the ITCZ at 1000 Cal yrs BP that decreased hurricane activity appears to have first promoted *C. erectus* expansion from 900 Cal yrs BP, but was soon followed by rapid *Pinus* expansion at 700 Cal yrs BP (Fig. 4H). A Buttonwood-dominated wetland also expanded in southeastern Abaco at ~900 Cal yrs BP⁵³. It appears that *C. erectus* populations already on the Bahamian landscape first benefited from the changing hydroclimate at 1000 Cal yrs BP. As regional subsidence between the anticyclonic flow and the easterlies concomitantly shifted southward with the ITCZ at 1000 Cal yrs BP, the resultant increased moisture delivery could have expanded suitable habitat in the topographic lows to the east of the study site. Thereafter, a slightly more northerly ITCZ from 700 to 500 Cal yrs BP is documented by the extratropical interhemispheric temperature anomaly and decreased accumulation rate of the Quelccaya Ice Cap (Fig. 4F), but not so far north as to return the northern Bahamas to arid conditions experienced from 2500 to 1000 Cal yrs BP. The southern ITCZ shift at 1000 Cal yrs BP seems to have initiated the necessary mesic conditions for *Pinus* expansion in both Abaco and Andros¹⁵.

From 600 to 300 Cal yrs BP, intense hurricane landfalls shifted to the North American northeast coast as recorded at Salt Pond, despite a more southerly ITCZ position. In the Bahamas, Blackwood records two intense events at ~500 Cal yrs BP, but a prominent active interval is recorded at Thatchpoint Bluehole (Fig. 1B)¹³. This is likely related to the lower intensity threshold for overwash deposition in the submerged bluehole (Thatchpoint) versus the subaerial sinkhole (Blackwood). The overwash record from Salt Pond in Massachusetts indicates one of greatest active intervals in the American Northeast in the last 2000 years. On the Abaco landscape, there is

a notable decline in *Pinus* synchronous with an increase in *C. erectus* at this time. This suggests expanded regional wetland development from increased moisture delivery, perhaps from the least exposure to the regional subsidence that currently promotes modern aridity on southern Bahamian islands⁴⁷.

These local vegetation changes are consistent with evidence for a southernmost ITCZ displacement during the late Holocene based on the greatest accumulation rates of the Quelccaya Ice Cap in the last 1300 years⁴³ and wettest period observed at Laguna Pumacocha in South America⁵⁴. A southerly ITCZ position should have hampered hurricane activity in the MDR. Indeed, Donnelly et al.⁹ attribute the increased hurricane strikes in the northeast between 600 and 300 Cal yrs BP to increased cyclogenesis or tropical transition of mid-latitude disturbances off the North American eastern seaboard in response to a western Atlantic warming event, which is likely related to a short-lived increase in overturning circulation⁵⁵. Given its geographic position, it appears that the northern Bahamas were also impacted by the increased storm activity on the northeastern American seaboard during this interval since Blackwood Sinkhole only records 2 intense events, but Thatchpoint Bluehole documents a more prolonged active interval from likely weaker storms just developing.

From 300 to 100 Cal yrs BP a noteworthy increase in intense hurricane landfalls occurred at Blackwood Sinkhole that is coincident with a decreased hurricane activity in New England. This active interval was observed previously at LPG, but higher sedimentation rates at LPG during the last several hundred years perhaps enhanced a bias for over-counting intense events in the last ~400 Cal yrs BP versus the earlier part of the record⁸. Due to its steady sedimentation rates, the reconstruction from BLWD-C2 suggests that this is a real feature of late Holocene hurricane activity. These results are at odds with other hurricane reconstructions that indicate that the Gulf of Mexico¹¹ and Yucatan coast¹² are inactive at this time. This interval occurs when the ITCZ should be more positioned in a more southerly position during the Little Ice Age. A high-resolution coral-based SST reconstruction from the northern Bahamas suggests increased SSTs in at least part of the Atlantic Warm Pool at this time⁵⁶, which may be impacting regional hurricane activity. These regional differences highlight the need for additional sub-decadal paleo hurricane records over the last millennium to more clearly resolve the regional timing and ocean-atmospheric forcing of paleo hurricane activity.

Implications

This study indicates that centennial-scale shifts in the ITCZ have likely played an important role in modulating intense hurricane landfalls along the western North Atlantic margin over the last 3000 years. However, the results further emphasize a pattern of zonal variability in paleo hurricane landfalls on millennial timescales⁹, as evidenced by active intervals in the Gulf of Mexico¹¹ versus western Atlantic margin (this study), which requires further evaluation. Considerable uncertainty still surrounds how North Atlantic hurricane activity will respond to anthropogenic influences on global climate⁵⁷, with some modeling results predicting an increase in activity in the Atlantic basin^{58,59}. Indeed, modern observations indicate that many variables influence hurricane intensity and frequency. As the Earth warms over this century, however, a northward shift in the thermal equator is predicted that will have an attendant ITCZ displacement^{60,61}. The results presented here then perhaps foreshadow a return to more persistent hurricane activity similar to a positive AMM-like state. The active interval of intense hurricane activity from 2500 to 1000 Cal yrs BP may provide an important analog for evaluating future hurricane and flooding risk along the now heavily-populated western North Atlantic margin.

Methods

Aerial photograph of Blackwood Sinkhole (Fig. 1) collected with a DJI Phantom 2 equipped with a GoPro Hero³ camera. Volumetric aliquots of sediment (2.5 cm³) at contiguous 5 mm intervals downcore were first rinsed over standard 32 μm and 63 μm meshes to isolate coarse silt- and sand-sized sediment fractions, respectively, and then desiccated overnight at 55°C. Each sieved sediment fraction was then heated to 550°C for 4.5 hours to combust organic particles. Finally, the remaining residue was re-weighed, and the volumetric quantity of coarse, inorganic sediment particles was obtained by difference (Sieve-first LOI method). The final measurement is mass (mg) of coarse particles >63 μm per cm³ of sediment [i.e.: $D_{>63 \mu\text{m}}$ (mg cm⁻³), not density]. The chronology was developed with twenty-one accelerator mass spectrometer ¹⁴C dates (see Table S1) on terrestrial plant macrofossils. Conventional ¹⁴C ages were calibrated to calendar years with INTCal13⁶². Near linear sedimentation described the topmost 110 cm of BLWD-C2 (least squares regression: $r^2=0.991$, $n = 11$ dates, Fig. S2), but *Bacon* (v2.2) generated the final age model from 110 to 0 cm using the IntCal13 calibration curve⁶³.

Sediment sub-samples ($n = 114$, 1.25 cm³) were processed for pollen analyses using standard palynological techniques at approximately 1 cm intervals throughout BLWD-C2. Two *Lycopodium* spore tablets (University of Lund, Batch No. 124961, ~12,500 spores each) were added to each sample to allow calculation of pollen and spore concentration. Samples were screened through 180 μm mesh screens to remove larger organics (i.e., leaves and wood). The samples were processed following standard techniques with 10 % HCl, 48% HF, 10% KOH,

followed by acetolysis mixture⁶⁴. The samples were then mounted on microscope slides, pollen grains were counted at 400-1000X magnification, and individual grains were identified with published taxonomic keys⁶⁴⁻⁶⁷ and the reference collection of P.L.F. An average of 360 pollen grains were counted in each sample. However, in the upper 31 cm where *Pinus* pollen dominates, at least 200 non-pine grains were counted and the sample mean equaled 492 grains (range: 433-673). From 32-109 cm, the mean was 320 grains (250-592). A final terrestrial pollen sum was calculated by excluding ferns, Cyperaceae, fungal spores and aquatic taxa due to the highly variable numbers and possible over representation.

Acknowledgments

This research was supported by NSF Awards: OCE-1519578, OCE-1356708, GSS-1118340. Technical and field support was provided by L. Lavold-Foote, D. Macdonald, S. Madsen, R. Sullivan, and T. Winkler. Comments from T. Cronin, J. Rodysill, and two anonymous reviewers improved the final manuscript. The data from BLWD-C2 are archived in the NOAA National climatic data center hurricane reconstruction database (<https://www.ncdc.noaa.gov/>). Any use of trade, firm, or product names is for descriptive purposes only and does not imply endorsement by the U.S. Government.

Author contributions

P.v.H., J.P.D., N.A.A and B.K. completed the fieldwork, P.v.H. completed the textural analysis, J.P.D and P.v.H. selected ¹⁴C dates and generated the age model, P.L.F. completed the pollen analysis, P.v.H., J.P.D., M.R.T., and P.L.F. interpreted the results, P.v.H. wrote the manuscript with contributions from all.

Competing Financial Interests

The authors declare no competing financial interests.

References

- 1 Gray, W. M. Global view of the origin of tropical disturbances and storms. *Month. Weath. Rev.* **96**, 669-700 (1968).
- 2 Goldenberg, S. B., Landsea, C. W., Mestas-Nunez, A. M. & Gray, W. M. The recent increase in Atlantic hurricane activity: causes and implications. *Science* **293**, 474-479 (2001).
- 3 Schneider, T., Bischoff, T. & Haug, G. H. Migrations and dynamics of the intertropical convergence zone. *Nature* **513**, 46-53 (2014).
- 4 Chiang, J. C. H. & Vimont, D. J. Analogous Pacific and Atlantic meridional modes of tropical atmosphere-ocean variability. *J. Clim.* **17**, 4143-4158 (2004).
- 5 Chang, P., Saravanan, R., Ji, L. & Hegerl, G. C. The effect of local sea surface temperatures on atmospheric circulation over the tropical Atlantic sector. *J. Clim.* **13**, 2195-2216 (2000).
- 6 Kossin, J. P. & Vimont, D. J. Understanding Atlantic Hurricane variability and trends. *Bull. Am. Meteorol. Soc.* **88**, 1767-1781 (2007).
- 7 Kossin, J. P., Camargo, S. J. & Sitkowski, M. Climate modulation of North Atlantic hurricane tracks. *J. Clim.* **23**, 3057-3076 (2010).
- 8 Donnelly, J. P. & Woodruff, J. D. Intense hurricane activity over the past 5,000 years controlled by El Niño and the West African Monsoon. *Nature* **447**, 465-468 (2007).
- 9 Donnelly, J. P. *et al.* Climate forcing of unprecedented intense-hurricane activity in the last 2,000 years. *Earth's Future*, doi:10.1002/2014EF000274 (2015).
- 10 Mylroie, J. E., Carew, J. L. & Moore, A. I. Blue holes: definitions and genesis. *Carb. Evapor.* **10**, 225-233 (1995).
- 11 Lane, P., Donnelly, J. P., Woodruff, J. D. & Hawkes, A. D. A decadal-resolved paleohurricane record archived in the late Holocene sediments of a Florida sinkhole. *Mar. Geol.* **287**, 14-30 (2011).
- 12 Denomee, K. C., Bentley, S. J. & Droxler, A. W. Climatic control on hurricane patterns: a 1200-y near-annual record from Lighthouse Reef, Belize. *Sci. Rep.* **4**, 7, doi:10.1038/srep03876 (2014).
- 13 van Hengstum, P. J. *et al.* Heightened hurricane activity on the Little Bahama Bank from 1350 to 1650 AD. *Cont. Shelf Res.* **86**, 103-115 (2014).
- 14 Gischler, E., Shinn, E. A., Oschmann, W., Fiebig, J. & Buster, N. A. A 1500-year Holocene Caribbean climate archive from the Blue Hole, Lighthouse Reef, Belize. *J. Coast. Res.* **24**, 1495-1505 (2008).
- 15 Kjellmark, E. Late Holocene climate change and human disturbance on Andros Island, Bahamas. *J. Paleolimnol.* **15**, 133-145 (1996).
- 16 Slayton, I. *A Vegetation History from Emerald Pond, Great Abaco Island, The Bahamas, Based on Pollen Analysis* MSc thesis, University of Tennessee, (2010).
- 17 Teeter, J. W. & Quick, T. J. Magnesium salinity relation in the saline late ostracode *Cyprideis americana*. *Geology* **18**, 220-222 (1990).
- 18 Knapp, K. R., Kruk, M. C., Levinson, D. H., Diamond, H. J. & Neumann, C. J. The international best track archive for climate stewardship (IBTrACS). *Bull. Am. Meteorol. Soc.* **91**, 364-376 (2009).

- 19 Holding, S. & Allen, D. M. From days to decades: numerical modeling of freshwater response to climate change stressor on small low-lying islands. *Hydrol. Earth Syst. Sci.* **19**, 933-949 (2015).
- 20 Rotzoll, K. & Fletcher, C. H. Assessment of groundwater inundation as a consequence of sea-level rise. *Nat. Clim. Chang.* **3**, 477-481 (2012).
- 21 Bowleg, J. & Allen, D. M. in *Climate change effects on groundwater resources: a global synthesis of findings and recommendations* (eds H. Treidel, J.L. Martin-Bordes, & J.J. Gurdek) 63-74 (Taylor and Francis, 2012).
- 22 Aguirre, B. Cancun under Gilbert: preliminary observations. *Int. J. Mass Emerg. Disast.* **7**, 69-82 (1989).
- 23 Lawrence, M. B. *et al.* Atlantic hurricane season of 1999. *Month. Weath. Rev.* **129**, 3057-3084 (2001).
- 24 Humblestone, S. in *The Abaconian* Vol. 7 4-5 (Marsh Harbour, 1999).
- 25 Franklin, J. L. *et al.* Annual Summary: Atlantic hurricane season of 2004. *Month. Weath. Rev.* **134**, 981-1025 (2004).
- 26 Lin, N., Lane, P., Emanuel, K. A., Sullivan, R. M. & Donnelly, J. P. Heightened hurricane surge risk in northwest Florida revealed from climatological-hydrodynamic modeling and paleorecord reconstruction. *J. Geophys. Res. D Atmos.* **119**, 8606-8623 (2014).
- 27 Woodruff, J. D., Donnelly, J. P., Mohrig, D. & Geyer, W. R. Reconstructing relative flooding intensities responsible for hurricane-induced deposits from Laguna Playa Grande, Vieques, Puerto Rico. *Geology* **36**, 391-394 (2009).
- 28 Milne, G. A. & Peros, M. Data-model comparison of Holocene sea-level change in the circum-Caribbean region. *Glob. Planet. Change* **107**, 119-131 (2013).
- 29 Woodruff, J. D., Donnelly, J. P., Emanuel, K. & Lane, P. Assessing sedimentary records of paleohurricane activity using modeled hurricane climatology. *Geochem. Geophys. Geosyst.* **9**, 12 (2008).
- 30 Bove, M. C., Elsner, J. B., Landsea, C. W., Niu, X. F. & O'Brien, J. J. Effect of El Niño on US landfalling hurricanes, revisited. *Bull. Am. Meteorol. Soc.* **79**, 2477-2582 (1998).
- 31 Chang, P., Ji, L. & Li, H. A decadal climate variation in the tropical Atlantic Ocean from thermodynamic air-sea interactions. *Nature* **386**, 516-518 (1997).
- 32 Vimont, D. J. & Kossin, J. P. The Atlantic Meridional Mode and hurricane variability. *Geophys. Res. Lett.* **34**, 5, doi:10.1029/2007GL029683 (2007).
- 33 Marcott, S. A., Shakun, J. D., Clark, P. U. & Mix, A. C. A reconstruction of regional and global temperature for the past 11,300 years. *Science* **339**, 1198-1201 (2013).
- 34 Haug, G. H., Hughen, K. A., Sigman, D. M., Peterson, L. C. & Röhl, U. Southward migration of the intertropical convergence zone through the Holocene. *Science* **293**, 1304-1308 (2001).
- 35 Lee-Thorp, J. A. *et al.* Rapid climate shifts in the southern African interior throughout the mid to late Holocene. *Geophys. Res. Lett.* **28**, 4507-4510 (2001).
- 36 Moy, C. M., Seltzer, G. O., Rodbell, D. T. & Anderson, D. M. Variability of El Niño/Southern Oscillation activity at millennial timescales during the Holocene. *Nature* **420**, 162-165 (2002).
- 37 Toomey, M. R., Curry, W. B., Donnelly, J. P. & van Hengstum, P. J. Reconstructing 7000 years of North Atlantic hurricane variability using deep-sea sediment cores from the western Great Bahama Bank. *Paleoceanography* **28**, 31-41 (2013).

- 38 Hodell, D. A. *et al.* Reconstruction of Caribbean climate change over the past 10,500
years. *Nature* **352**, 790-793 (1991).
- 39 Caffrey, M. A., Horn, S. P., Orvis, K. H. & Haberyan, K. A. Holocene environmental
change Laguna Saladilla, coastal north Hispaniola. *Palaeogeog. Palaeoclim. Palaeoecol.*
4346, 9-22 (2015).
- 40 Higuera-Gundy, A. *et al.* A 10,300 14C yr record of climate and vegetation change from
Haiti. *Quat. Res.* **52**, 159-170 (1999).
- 41 Waldeab, S., Schneider, R. R., Kölling, M. & Wefer, G. Holocene African droughts relate
to eastern equatorial cooling. *Geology* **33**, 981-984 (2005).
- 42 Mann, M. E., Woodruff, J. D., Donnelly, J. P. & Zhang, Z. Atlantic hurricanes and climate
over the past 1,500 years. *Nature* **460**, 880-885 (2009).
- 43 Thompson, L. G. *et al.* Annually resolved ice core records of tropical climate variability
over the past 1800 years. *Science* **340**, 945-950 (2013).
- 44 Hodell, D. A., Brenner, M. & Curtis, J. H. Terminal Classic drought in the northern Maya
lowlands inferred from multiple sediment cores in Lake Chichancanab (Mexico). *Quat.*
Sci. Rev. **24**, 1413-1427 (2005).
- 45 Lane, C. S., Horn, S. P. & Kerr, M. T. Beyond the Mayan Lowlands: impacts of the
Terminal Classic Drought in the Caribbean Antilles. *Quat. Sci. Rev.* **86**, 89-98 (2014).
- 46 Gregory, B. R. B., Peros, M., Reinhardt, E. G. & Donnelly, J. P. Middle-late Holocene
Caribbean aridity inferred from foraminifera and elemental data in sediment cores from
two Cuban lagoons. *Palaeogeog. Palaeoclim. Palaeoecol.* **426**, 229-241 (2015).
- 47 Jury, M., Malmgren, B. A. & Winter, A. Subregional precipitation climate of the
Caribbean and relationships with ENSO and NAO. *J. Geophys. Res.* **112**, 11 (2007).
- 48 Gamble, D. W. & Curtis, S. Caribbean precipitation: a review, model and prospect. *Prog.*
Phys. Geog. **32**, 265-276 (2008).
- 49 Dima, I. M. & Wallace, J. M. On the seasonality of the Hadley Cell. *J. Atmos. Sci.* **60**,
1522-1526 (2003).
- 50 Hastings, A. K., Krigbaum, J., Steadman, D. W. & Albury, N. A. Domination by Reptiles
in a Terrestrial Food Web of the Bahamas Prior to Human Occupation. *J. Herpet.* **48**, 380-
388 (2014).
- 51 Soto-Centeno, J. A. & Steadman, D. W. Fossils reject climate change as the cause of
extinction in Caribbean bats. *Sci. Rep.* **5**, doi:0.1038/srep07971 (2015).
- 52 Steadman, D. W. *et al.* Exceptionally well preserved late Quaternary plant and vertebrate
fossils from a blue hole on Abaco, The Bahamas. *Proc. Nat. Acad. Sci. U.S.A.* **104**, 19897-
19902 (2007).
- 53 Steadman, D. W. *et al.* Late-Holocene faunal and landscape change in the Bahamas.
Holocene **24**, 220-230 (2014).
- 54 Bird, B. W. *et al.* A 2,300-year-long annually resolved record of the South American
summer monsoon from the Peruvian Andes. *Proc. Nat. Acad. Sci. U.S.A.* **108**, 8583-8588
(2011).
- 55 Rahmstorf, S. *et al.* Exceptional twentieth-century slowdown in Atlantic Ocean
overturning circulation. *Nat. Clim. Chang.* **5**, 475-480 (2015).
- 56 Saenger, C., Cohen, A. L., Oppo, D. W., Halley, R. B. & Carilli, J. E. Surface-temperature
trends and variability in the low-latitude North Atlantic since 1552. *Nat. Geosci.* **2**, 492-
495 (2009).

- 57 Knutson, T. R. *et al.* Tropical cyclone and climate changes. *Nat. Geosci.* **3**, 157-163 (2010).
- 58 Emanuel, K. A. Downscaling CMIP5 climate models shows increased tropical cyclone activity over the 21st century. *Proc. Nat. Acad. Sci. U.S.A.* **110**, 12219-12224, doi:10.1073/Pnas.1301293110 (2013).
- 59 Doi, T., Vecchi, G. A., Rosati, A. J. & Delworth, T. L. Response to CO2 doubling of the Atlantic Hurricane main development region in a high-resolution climate model. *Am. Meteorol. Soc.* **26**, 4322-4334 (2013).
- 60 Broecker, W. S. & Putnam, A. E. Hydrologic impacts of past shifts of thermal equator offer insight into those to be produced by fossil fuel CO2. *Proc. Nat. Acad. Sci. U.S.A.* **110**, 16710-16715 (2013).
- 61 Ceppi, P., Hwang, Y.-T., Liu, X., Frierson, D. M. W. & Hartmann, D. L. The relationship between the ITCZ and the southern hemispheric eddy-driven jet. *J. Geophys. Res. D Atmos.* **118**, 5136-5146 (2013).
- 62 Reimer, P. J. *et al.* IntCal13 and Marine13 radiocarbon age calibration curves 0-50,000 years Cal BP. *Radiocarbon* **55**, 1869-1887 (2013).
- 63 Blaauw, M. & Christen, A. Flexible paleoclimate age-depth models using an autoregressive gamma process. *Bay. Anal.* **6**, 457-474 (2011).
- 64 Faegri, K. & Iverson, J. in *Textbook of Pollen Analysis* (eds K. Faegri, P.E. Kaland, & K. Krzywinski) (John Wiley, 1989).
- 65 Bertrand, R. Pollen from four common New World mangroves in Jamaica. *Grana* **22**, 147-151 (1983).
- 66 Synder, T., Chiantello, J., Kjellmark, E. & Baumgardner, K. *Key to Pollen of the Bahamas*, <<http://www.pollen.mtu.edu>> (2007), (Date of access: 18/01/2016).
- 67 Willard, D. A. *et al.* Atlas of pollen and spores of the Florida Everglades. *Palynology* **28**, 175-227 (2004).

Figures & Captions Captions

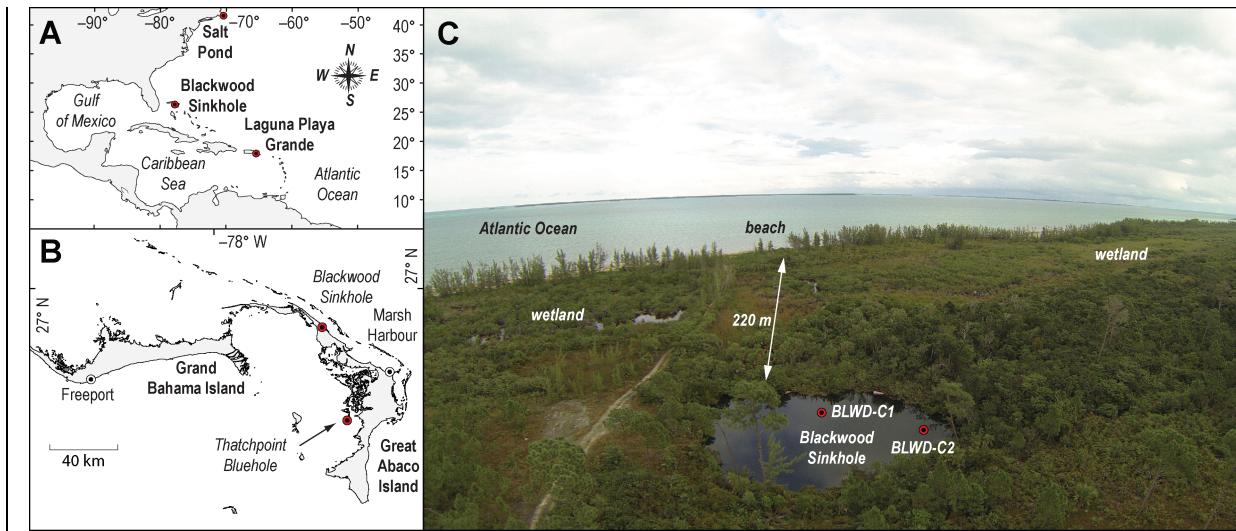


Figure 1. **A:** The western North Atlantic region noting the location of Blackwood Sinkhole on the Little Bahama Bank, Laguna Playa Grande in Puerto Rico, and Salt Pond in Massachusetts, USA. **B:** Islands on the Little Bahama Bank, and the position of Blackwood Sinkhole relative to Thatchpoint Bluehole. **C:** Aerial photograph of Blackwood Sinkhole facing a northeasterly direction. Maps in A and B modified with permission after¹³.

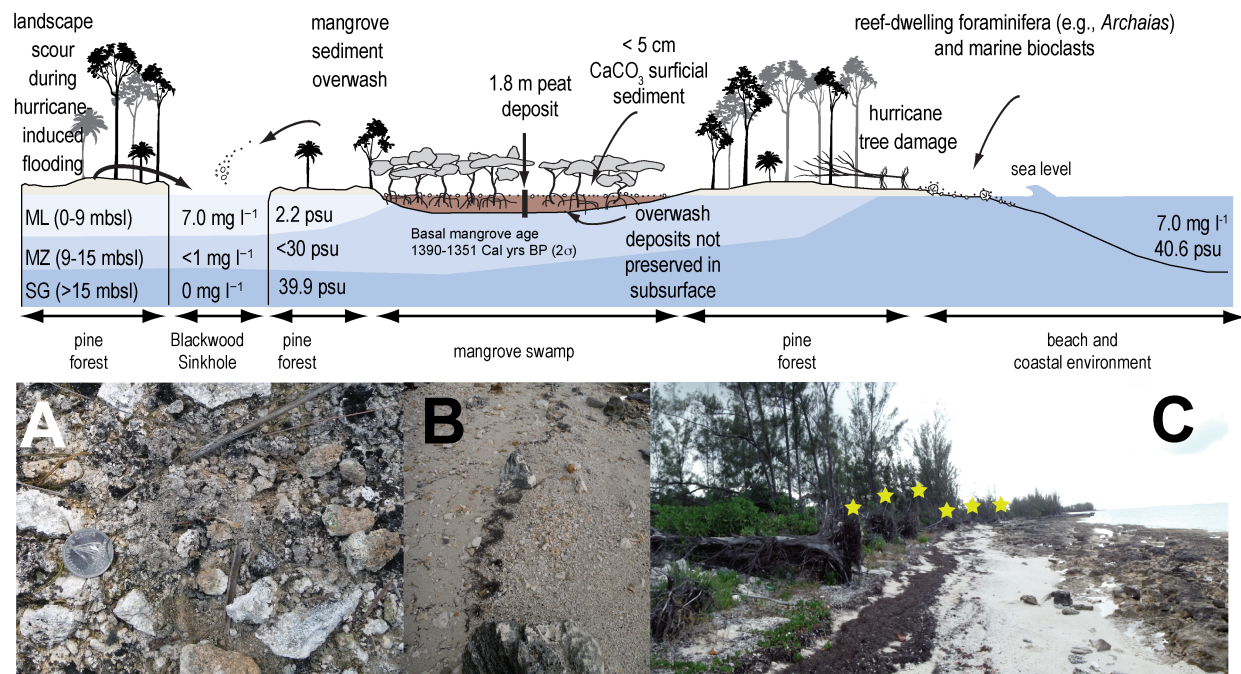


Figure 2. A conceptual model of the landscape surrounding Blackwood Sinkhole that illustrates the local sediment supply, and the likely processes that are promoting overwash into the sinkhole during an intense hurricane event (not to horizontal or vertical scale). Blue shading refers to different groundwater masses in the sinkhole, with their respective differences in dissolved oxygen and salinity (ML: meteoric lens, MZ: mixing zone, SG: saline groundwater). The peat in the adjacent mangrove swamp did not contain overwash deposits, and basal peat sediments were aged to ~1350 years ago (Table S1). Photographs: **(A)** The surficial sediment on the surrounding terrestrial landscape (the location of S1 in Fig. S4A) contains angular carbonate particles (weathered karst fragments) and no shell material. These terrestrial sediment particles are similar to the coarse-grained particles in the overwash deposits preserved in the sediment core from Blackwood Sinkhole (BLWD-C2). **(B)** In contrast, coarse sediment ($> 63 \mu\text{m}$, 5cm^3) on the adjacent beach contains rounded marine mollusk fragments, foraminiferal assemblages dominated by reef-dwelling foraminifera (*Archaias angulatus*), and coral fragments. **(C)** A row of toppled trees (yellow stars, *Casuarina* sp.) from a previous storm, just behind the high-tide wrack line. The diameter of the quarter is 24.2 mm.

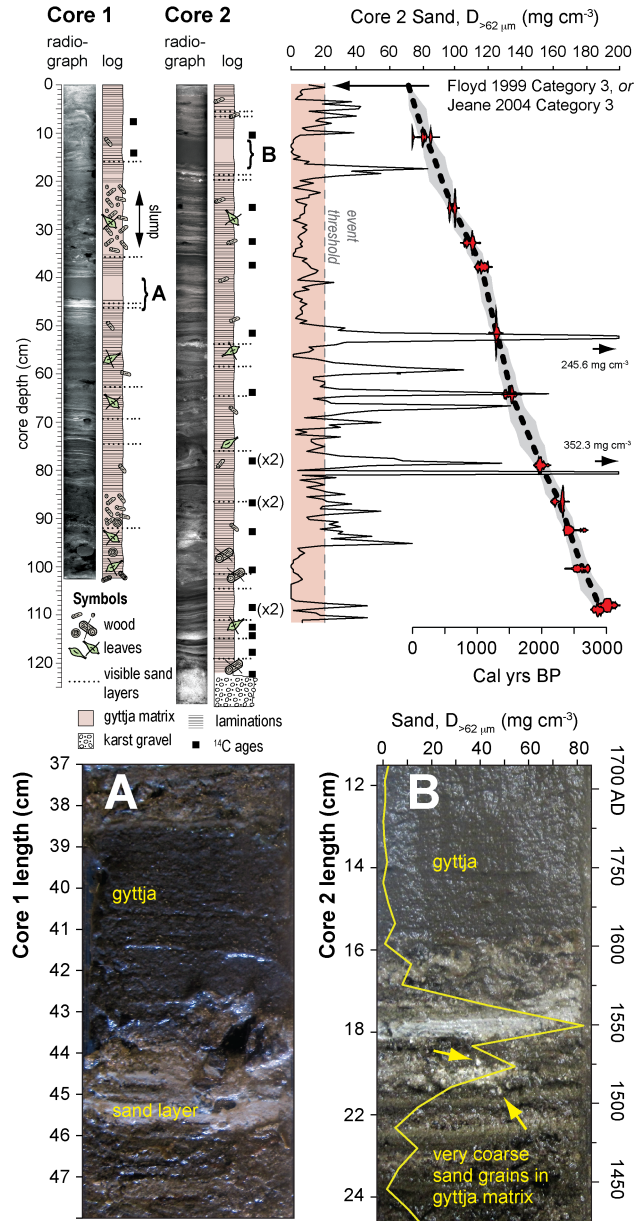


Figure 3. Core photographs, X-radiographs, generalized lithology, and position of radiocarbon dates (Table S1). The bottom panels (A, B) compare a salient algal gyttja horizon, laminations, and coarse layers between the cores. The top and bottom sand layers in panel B were deposited at 1549 AD (2σ : 1402 to 1715 AD) and 1524 AD (2σ : 1378.9 to 1698.8 AD), respectively.

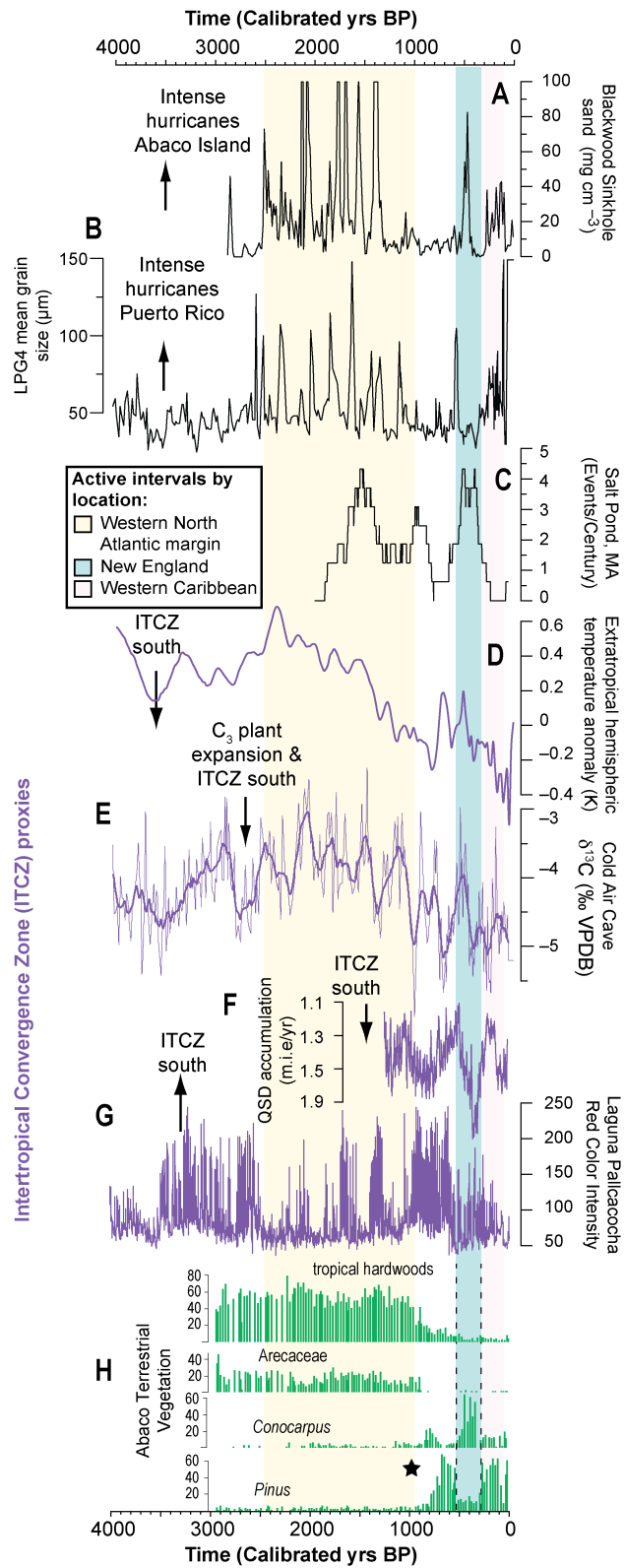


Figure 4. A: Sand deposition into Blackwood Sinkhole from BLWD-C2, B: intense hurricane overwash deposits, Puerto Rico⁸, C: Intense hurricane events at Salt Pond, Massachusetts⁹, D:

Northern-to-Southern hemisphere temperature anomaly^{3,33}, **E**: Raw (light purple) and 100-pt mean (dark purple) of $\delta^{13}\text{C}$ measurements from speleothem T7 from Cold Air Cave, South Africa³⁵, **F**: Quelccaya Ice Cap accumulation rate, Peru⁴³, **G**: Laguna Pallcacocha red color intensity provides evidence for periods of increased intense precipitation, Ecuador³⁶, **H**: pollen-based evidence for vegetation changes on Great Abaco Island. Star denotes oldest radiocarbon dated human remains yet recovered from northern Bahamas⁵². Zero on the horizontal axis is 2000 CE.

Online Sedimentary Information

Blackwood Sinkhole presents as a classic sinkhole basin with a stratified water column. The sinkhole provides a porthole into the local coastal aquifer, where the upper meteoric lens is stratified from the anoxic saline groundwater (Fig. S1). The anoxic conditions at the sediment water interface enhances sediment preservation by limiting the action of bioturbating organisms (e.g., worms, bivalves). Sedimentation rate at the site of BLWD-C2 has been nearly constant over the last 3000 years (Fig. S2, Table S1). Likely sediment sources include organic matter from primary production, authigenic calcium carbonate precipitation, and erosional products from the adjacent landscape. Despite the proximity of the sinkhole to the beach, classic beach sedimentary particles (rounded marine mollusks, reef-dwelling benthic foraminifera) were not found in the coarse layers of BLWD-C2 (Fig. S3).

One sediment push core was collected from the adjacent mangrove swamp, which sampled the entire peat stratigraphy to the eolianite bedrock (Fig. S4, BLWD-MC1, 26.799067°, -77.422352°). Before coring, we used a sediment probing staff to map the peat-eolianite contact in the subsurface to ensure we collected the most complete and expansive stratigraphic succession from this area. We also excavated several small pits in the mangrove peat. As such, the purpose of this additional sampling was to answer the following questions that are related to the overall sediment reconstruction from BLWD-C2: (1) are any overwash deposits preserved in the mangrove peat, and (2) how does the constant sedimentation rate at Blackwood Sinkhole over the last ~3000 years relate to timing of colonization of the mangrove swamp in the adjacent eolianite interdune swale?

The radiocarbon age of a terrestrial plant macrofossil at the base of the mangrove peat succession (BLWD-MC1: 108-110 cm) suggests that sedimentation in the interdune swale initiated at >1350 Cal yrs BP (Table S1). This is within ~200 years of the increase in *Conocarpus* pollen preserved in BLWD-C2, and likely expansion of the wetland environment adjacent to Blackwood Sinkhole. These results suggest that the near linear sedimentation at the coring site of BLWD-C2 has been maintained by several factors (i.e., not just organic sediment derived from mangroves) over the late Holocene. Indeed, additional cores are required from Blackwood Sinkhole to determine the complete impact of mangrove development on the spatial stratigraphic architecture in Blackwood Sinkhole over the late Holocene, which is beyond the scope of the present study.

Note: Any use of trade, firm, or product names is for descriptive purposes only and does not imply endorsement by the U.S. Government.

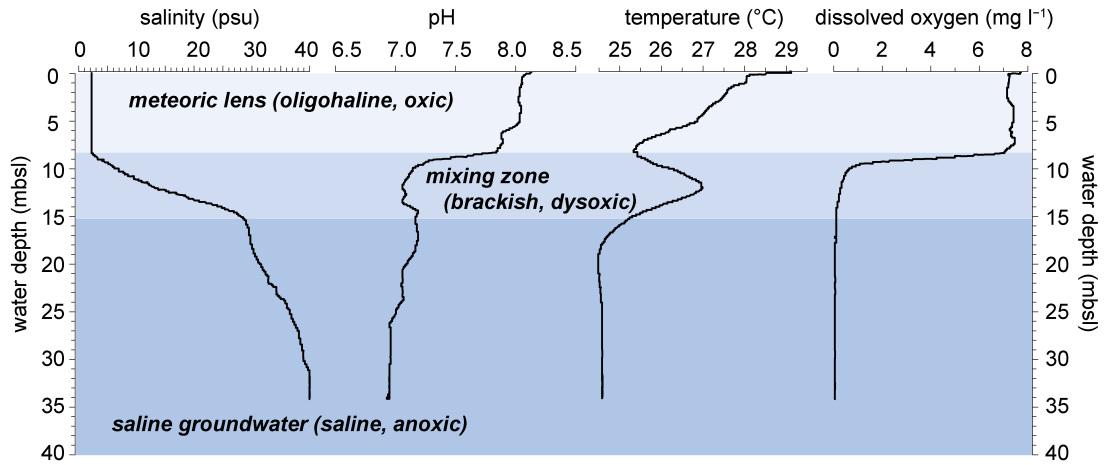


Figure S1. Vertical hydrographic profiles for Blackwood Sinkhole, measured on the 25 May 2014 with a YSI EXO1 multi-parameter sonde.

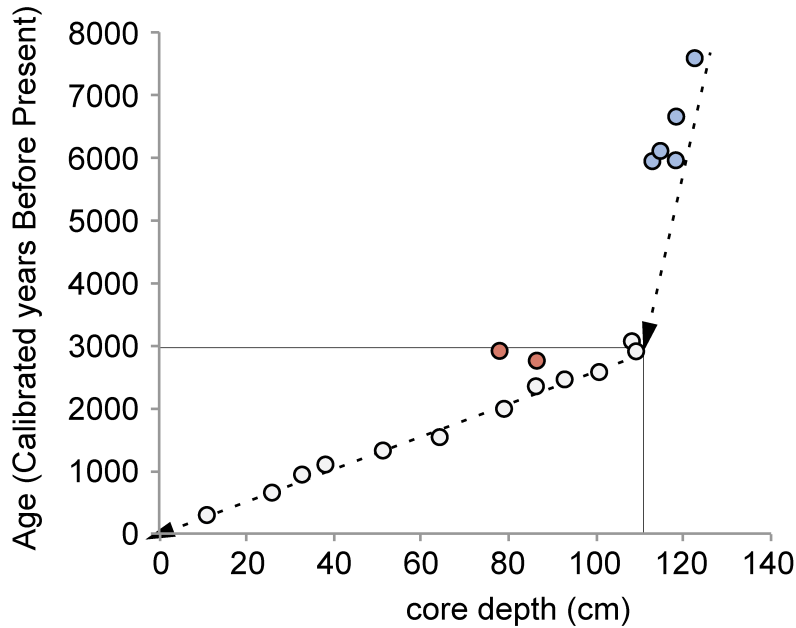


Figure S2. Age-depth plot of radiocarbon results from BLWD-C2. The dates plotted are the highest probability 1σ calibrated result from Calib 7.0. Grey data points plotted were used to generate a final age model in *Bacon* (v2.2) using Bayesian statistical methods (see Fig. 2 in article). The red data points are likely terrestrial plant macrofossils that resided on the terrestrial surface for several hundred years before becoming deposited into Blackwood Sinkhole, and younger results were obtained from other co-stratigraphic terrestrial plant macrofossils (e.g., 86 to 87 cm). Blue data points indicate that sedimentation in Blackwood Sinkhole was negligible or episodic (hiatus between 3.0 and 6.0 ka?) prior to 3000 Cal yrs BP, after which sedimentation was linear and continuous through the late Holocene (least squares regression: $r^2=0.991$, $n = 11$ AMS dates). Note: the size of datapoint plotted above mostly encompasses the uncertainty for highest probability 1σ calibration result, see Table S1 for complete radiocarbon calibration results.

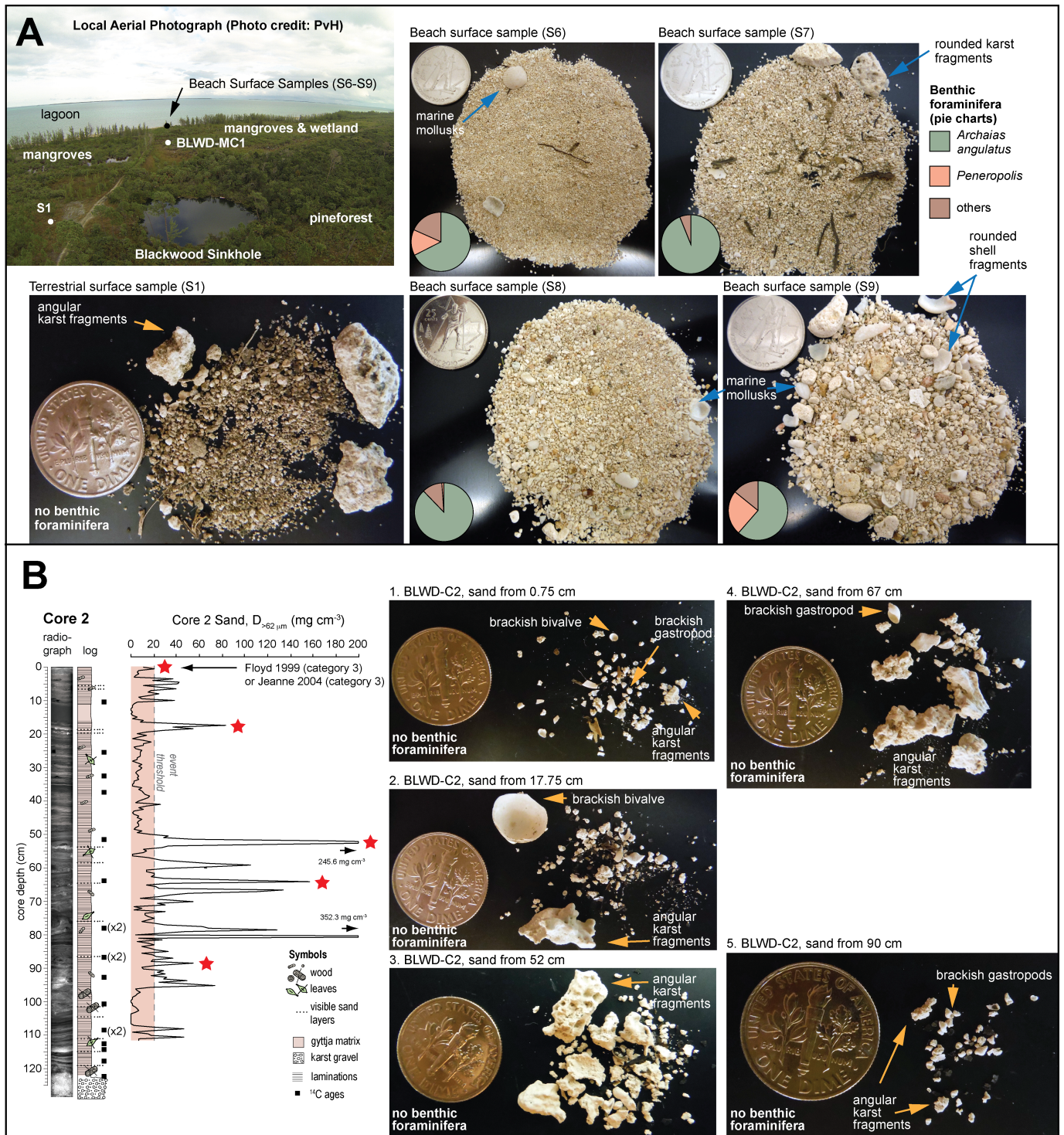


Fig S3. A: An aerial photograph in the top-left depicts the location of surface sediment samples, and a core collected from the deepest location in the adjacent wetland (BLWD-MC1, Table S1). **B:** Detailed analysis of the coarse sediment particles preserved in five coarse-grained layers in BLWD-C2 (red stars, sieved at $>63\ \mu m$, $1.25\ cm^3$ sediment volume). The coarse-grained layers are characterized by highly angular and weathered carbonate fragments, whole and articulated brackish mollusks (bivalves, gastropods), and no benthic foraminifera. In the multiple samples examined under stereomicroscopy for microfossils from BLWD-C2, only rare mangrove benthic

foraminiferal taxa (e.g., *Rosalina globularis*, *Jadammina macrescens*) or brackish testate amoebae were observed (e.g., *Centropyxis aculeata*), which are not in situ because these taxa cannot survive in the anoxic state of the bottom water (saline groundwater). These results indicate that the adjacent terrestrial and wetland environments are the primary source of coarse-grained sediment deposited into Blackwood Sinkhole during intense flooding events. The diameter of an American dime is 17.9 mm, and the diameter of a Canadian quarter is 23.8 mm.

Table S1 (Following Page). Radiocarbon results for core BLWD-C1 and BLWD-C2 (enclosed on [page 6](#) of online supplement). Note that the radiocarbon results from the leaf fragment from BLWD-C2 77.5 to 78 cm, and the twig from BLWD-C2 86.0 to 86.5 cm were excluded from the final Bacon Age model as they were systematically older than the radiocarbon results on material at the same or nearby stratigraphic levels.

Index No.	Lab number	Core	Core interval (cm)	Material	Conventional ¹⁴ C age	Fraction Modern (Δ ¹⁴ C)	δ ¹³ C _{org} (‰)	Calibrated 1σ ranges (probability)	Calibrated 2σ ranges (probability)
1	OS-92769	BLWD-C2	10.5 to 11 cm	single leaf	205 ± 25	0.975 ± 0.0032	-27.7	0 to 10 (0.1714) 150 to 173 (0.4501) 178 to 184 (0.0586) 267 to 301 (0.2965)	0 to 15 (0.1552) 145 to 214 (0.5482) 267 to 301 (0.2965)
2	OS-92835	BLWD-C2	25 to 26 cm	leaf fragments	680 ± 25	0.9188 ± 0.0031	-27.76	570 to 580 (0.2671) 651 to 670 (0.7328)	563 to 59 (0.3392) 639 to 677 (0.6607)
3	OS-92771	BLWD-C2	32.5 to 33 cm	leaves	1000 ± 30	0.8828 ± 0.0032	-27.7	834 to 841 (0.0707) 909 to 958 (0.9293)	798 to 815 (0.0601) 822 to 869 (0.1997) 898 to 967 (0.7401)
4	OS-90975	BLWD-C2	37.5 to 38 cm	twig	1160 ± 25		-27.24	1007 to 1029 (0.2186) 1053 to 1092 (0.4764) 1106 to 1136 (0.2632) 1162 to 1167 (0.0417)	983 to 1034 (0.2638) 1048 to 1151 (0.6654) 1156 to 1171 (0.0706)
5	OS-90976	BLWD-C2	51.25 to 51.75 cm	twig	1380 ± 25		-27.58	1286 to 1307 (1.)	1277 to 1336 (1.)
6	OS-90995	BLWD-C2	64 to 64.5 cm	twig	1630 ± 30	0.8166 ± 0.0032	-27.21	1420 to 1434 (0.1037) 1440 to 1461 (0.1864) 1513 to 1563 (0.7097)	1415 to 1572 (0.9473) 1581 to 1602 (0.0526)
7	OS-89451	BLWD-C2	77.5 to 78 cm	leaf	2780 ± 35		-28.88	2810 to 2813 (0.0273) 2845 to 2929 (0.9102) 2936 to 2945 (0.0624)	2787 to 2957 (1.)
8	OS-90977	BLWD-C2	78.75 to 79.25 cm	twig	2030 ± 25		-29.1	1934 to 1937 (0.0254) 1945 to 2003 (0.9413) 2029 to 2033 (0.0332)	1899 to 1912 (0.0225) 1921 to 2059 (0.9752) 2099 to 2101 (0.0021)
9	OS-90978	BLWD-C2	86 to 86.5 cm	twig	2610 ± 35		-27.55	2729 to 2760 (1.)	2551 to 2555 (0.0034) 2618 to 2633 (0.03082) 2705 to 2787 (0.9657)
10	OS-92771	BLWD-C2	86 to 87 cm	twigs	2290 ± 25	0.752 ± 0.0023		2313 to 2347 (1.)	2183 to 2234 (0.2192) 2306 to 2350 (0.7807)
11	OS-92772	BLWD-C2	92 to 93 cm	twig fragments	2400 ± 30	0.7412 ± 0.0026		2353 to 2376 (0.2327) 2384 to 2459 (0.7672)	2346 to 2493 (0.9030) 2600 to 2609 (0.0116) 2640 to 2680 (0.0852)
12	OS-90994	BLWD-C2	100 to 101 cm	twig	2520 ± 35	0.7303 ± 0.0032	-15.79	2503 to 2530 (0.1661) 2537 to 2594 (0.4102) 2614 to 2637 (0.1844) 2696 to 2727 (0.2391)	2487 to 2742 (1.)
13	OS-90996	BLWD-C2	108 to 108.5 cm	twig	2890 ± 35	0.6974 ± 0.0027	-17.29	2962 to 3072 (1.)	2891 to 2903 (0.01395) 2924 to 3084 (0.8392) 3086 to 3159 (0.1467)
14	OS-89450	BLWD-C2	108.75 to 109.25 cm	twig	2790 ± 30		-17.59	2853 to 2928 (0.9729) 2939 to 2941 (0.0270)	2794 to 2831 (0.0910) 2838 to 2960 (0.9089)
15	OS-92773	BLWD-C2	112.5 to 113 cm	bulk sediment	5160 ± 35	0.5261 ± 0.0024	-31.7	5900 to 5942 (0.8521) 5972 to 5985 (0.1478)	5761 to 5809 (0.1027) 5886 to 5992 (0.8972)
16	OS-92832	BLWD-C2	114.5 to 115 cm	bulk sediment	5280 ± 35	0.5181 ± 0.0021	-32.33	5991 to 6028 (0.2890) 6044 to 6068 (0.1698) 6076 to 6118 (0.3330) 6150 to 6177 (0.2079)	5943 to 5971 (0.0879) 5985 to 6133 (0.7089) 6136 to 6182 (0.2030)
17	OS-92833	BLWD-C2	117.8 to 118.3 cm	bulk sediment	5830 ± 35	0.4836 ± 0.0022	-31.41	6566 to 6588 (0.1757) 6602 to 6614 (0.0694) 6615 to 6677 (0.6977) 6705 to 6715 (0.0570)	6538 to 6737 (1.)
18	OS-90997	BLWD-C2	117.75 to 118.25 cm	twig	5160 ± 35	0.5263 ± 0.0024	-28.48	5900 to 5942 (0.8521) 5972 to 5985 (0.1478)	5761 to 5809 (0.1027) 5886 to 5992 (0.8972)
19	OS-92834	BLWD-C2	122.0 to 122.5 cm	wood fragments	6700 ± 35	0.434 ± 0.002	-29.74	7515 to 7537 (0.3258) 7562 to 7594 (0.6533) 7603 to 7605 (0.0207)	7494 to 7622 (0.9899) 7643 to 7650 (0.0100)
20	OS-92767	BLWD-C1	7 to 8 cm	leaf	275 ± 25	0.9665 ± 0.0032	-27.8	293 to 317 (0.5881) 397 to 422 (0.4118)	157 to 165 (0.0203) 285 to 330 (0.5086) 359 to 429 (0.4710)
21	OS-92768	BLWD-C1	14.5 to 15 cm	leaf fragments	140 ± 25	0.9828 ± 0.003	-25.1	0 to -1 (0.0083) 12 to 33 (0.1896) 73 to 100 (0.1871) 103 to 115 (0.0809) 136 to 149 (0.1150) 187 to 225 (0.2792) 254 to 270 (0.1395)	0 (0.0059) 7 to 40 (0.1680) 60 to 119 (0.2560) 122 to 152 (0.1256) 171 to 233 (0.2791) 241 to 280 (0.1651)